Available online at www.sciencedirect.com
SCIENCE DIRECT®
Journal of Solid State Chemistry 173 (2003) 13–19
JOURNAL OF SOLID STATE CHEMISTRY
http://elsevier.com/locate/jssc

High-pressure structure of Li_2CO_3

Andrzej Grzechnik,[a,*] Pierre Bouvier,[b,1] and Luca Farina[c]

[a] *Max-Planck-Institut für Festkörperforschung, Heisenbergstrasse 1, Stuttgart D-70569, Germany*
[b] *European Synchrotron Radiation Facility, B.P. 220, Grenoble cedex F-38043, France*
[c] *Dipartimento di Chimica Fisica e Inorganica, Università di Bologna, Viale Risorgimento 4, Bologna I-40136, Italy*

Received 16 August 2002; received in revised form 8 December 2002; accepted 19 December 2002

Abstract

The high-pressure behavior of Li_2CO_3 is studied up to 25 GPa with synchrotron angle-dispersive powder X-ray diffraction in diamond anvil cells and synthesis using a multi-anvil apparatus. A new non-quenchable hexagonal polymorph ($P6_3/mcm$, $Z = 2$) occurs above 10 GPa with carbonate groups in a staggered configuration along the c-axis—$a = 4.4568(2)$ Å and $c = 5.1254(6)$ Å at 10 GPa. Two columns of face-shared distorted octahedra around the Li atoms are linked through octahedral edges. The oxygen atoms are coordinated to one carbon atom and four lithium atoms to form a distorted square pyramid. Splittings of X-ray reflections for the new polymorph observed above about 22 GPa under non-hydrostatic conditions arise from orthorhombic or monoclinic distortions of the hexagonal lattice. The results of this study are discussed in relation to the structural features found in other Me_2CO_3 carbonates (*Me*: Na, K, Rb, Cs) at atmospheric conditions.

1. Introduction

Alkali metal carbonates are used as non-metallic catalysts for a synthesis of diamonds [1–3]. Unlike in traditional metal–carbon systems, in which the synthesis is carried out under highly reducing conditions in the presence of a methane–hydrogen fluid, crystallization of diamond in carbonate–carbon systems occurs in the presence of a H_2O–CO_2-rich fluid [4]. The catalytic activity of the carbonates diminishes in the sequence $Li_2CO_3 \gg Na_2CO_3 > K_2CO_3 > Cs_2CO_3$ [5]. The rate of synthesis reaction and the number of diamond nuclei decrease with the increase of cation radii, $Li^+ \rightarrow Na^+ \rightarrow K^+ \rightarrow Cs^+$. The carbonate catalysts offer a possibility of diamond formation in a wide range of redox conditions [4].

One of the basic issues in the efficient use of the non-metallic catalysts is whether their activity is influenced by their chemical and structural instabilities [6]. For instance, it is known that the rate of decomposition for lithium and sodium carbonates is greatly enhanced when carbon black is added [7]. No such information is available in the literature regarding this phenomenon occurring under compression. There is also no data on the pressure-induced phase transitions in any of the alkali metal carbonates. This study reports on the high-pressure behavior of lithium carbonate, Li_2CO_3, up to 25 GPa as studied with synchrotron angle-dispersive powder X-ray diffraction in diamond anvil cells and synthesis using a multi-anvil apparatus. The results are discussed in relation to the structural features found in other Me_2CO_3 carbonates (*Me*: Na, K, Rb, Cs) at atmospheric conditions.

2. Experimental

The Li_2CO_3, Li_2O, and black Pt materials were obtained from Aldrich. Angle-dispersive powder X-ray diffractograms ($\lambda = 0.3738$ Å) at high pressures were measured on the ID30 beamline at the European Synchrotron Radiation Facility, Grenoble. Patterns were collected using the MAR 345 image plate detector. The images were integrated using the program FIT2D [8] to yield intensity versus 2θ diagrams. The powder sample of pure Li_2CO_3 was loaded into diamond anvil

*Corresponding author. Fax: +49-711-689-1010.
E-mail address: andrzej@servix.mpi-stuttgart.mpg.de (A. Grzechnik).
[1] Present address: Laboratoire d'Electrochimie et de Physicochimie des Materiaux et des Interfaces, UMR 5631-CNRS, 1130 Rue de la Piscine, BP 75, F-38402 Saint Martin d'Heres cedex, France.

0022-4596/03/$ - see front matter © 2003 Elsevier Science (USA). All rights reserved.
doi:10.1016/S0022-4596(03)00053-7

cells either with no pressure medium or with paraffin oil. For laser annealing experiments, the stoichiometric mixture of Li_2CO_3 and Li_2O was loaded into a diamond anvil cell together with black Pt (about 1wt%). The mixture of the oxides, that have low IR absorption, was indirectly heated by irradiating black Pt with a YAG laser. After *off-line* laser annealing with estimated temperatures below 1273 K, X-ray diffraction patterns of the samples quenched to room temperature were collected at different pressures. The ruby luminescence method [9] was used for pressure calibration.

The high-pressure high-temperature syntheses were performed with a Walker-type multi-anvil apparatus [10]. The pressure medium consisted of a MgO(95wt%)–Cr_2O_3(5wt%) octahedron (18 mm), and pressure was applied by eight tungsten carbide cubes with corners truncated to triangular faces (11 mm). The samples of pure Li_2CO_3, loaded into Pt ampoules (2 mm in diameter and 3.5 mm in height), were pressurized to 11 GPa and then heated at different temperatures. The heaters, isolated from the ampoules by MgO sleeves, were made of $LaCrO_3$ ceramics. Temperatures at the samples were measured with W-26%Re/W-5%Re thermocouples. Pressure calibration is discussed in detail in Ref. [10]. The recovered products to ambient conditions were examined by powder X-ray diffraction with the STOE-STADI diffractometer (equipped with a PSD detector) in Debye–Scherrer scan mode using Cu$K\alpha_1$ radiation.

3. Crystal structures of alkali metal carbonates at ambient pressure

The crystal structure of Li_2CO_3 ($C2/c, Z = 4$) is built of planar CO_3^{2-} anions and lithium atoms tetrahedrally coordinated to oxygens [11]. All the atoms of the Li_2CO_3 formula unit lie in the same plane. The carbonate ions are nearly staggered with the carbon atoms in a zigzag configuration along the *c*-axis. Pairs of LiO_4 tetrahedra sharing their edges are connected by vertices to the carbonate anions. One of the oxygen atoms (O1) is coordinated to the carbon atom and two lithium atoms, while the second oxygen (O2) is coordinated by the carbon atom and three lithium atoms. The C–O1 and C–O2 bond lengths are 1.270 and 1.286 (2×) Å, respectively, and the Li–O distances are 1.887 (Li–O2), 1.952 (Li–O2), 1.975 (Li–O2), and 2.025 (Li–O2) Å.

The monoclinic space groups of γ-K_2CO_3, Rb_2CO_3, Cs_2CO_3 (all $P2_1/c, Z = 4$), β-K_2CO_3 ($C2/c, Z = 4$), and β-/γ-Na_2CO_3 ($C2/m$, $Z = 4$) are subgroups of the common supergroup $Cmcm$ ($Z = 4$) [12]. The aristotype of all these structures is represented by α-Na_2CO_3 and α-K_2CO_3 crystallizing in space group $P6_3/mmc$ ($Z = 2$). The phase transition $P6_3/mmc - C2/m$ ($\alpha - \beta$) in Na_2CO_3 at 754 K is second-order proper ferroelastic with the order parameter being the shear strain ε_5 [13]. In the crystal structure of the high-temperature hexagonal α phase, one of the sodium atoms is octahedrally coordinated to the oxygen atoms, and the NaO_6 octahedra form face-sharing columns along [001]. The columns are interconnected by the carbonate groups. The second sodium atom is located in a site directly above the carbon atom along the *c*-axis. The individual columns of the NaO_6 octahedra do not distort significantly as a result of the $\alpha - \beta$ phase transition, but neighboring columns, hinged by the carbonate groups which rotate in phase with the shear strain, move along [001] with respect to each other. The γ modification ($C2/m$, $Z = 4$) is incommensurate with a periodic bending of the octahedral columns and with the carbonate anions acting as freely hinging connections [14]. The main difference between the structures of β-K_2CO_3 ($C2/c, Z = 4$) and of the hexagonal aristotype is that the CO_3^{2-} anions are rotated around one of the C–O bonds in β-K_2CO_3 to lower the symmetry of the crystal lattice [15]. The $P2_1/c$ ($Z = 4$) modifications of γ-K_2CO_3, Rb_2CO_3, and Cs_2CO_3 are superstructures of β-K_2CO_3.

4. Results and discussion

Selected powder X-ray patterns of Li_2CO_3 upon compression with paraffin oil as a pressure medium are shown in Fig. 1. Up to about 6 GPa, the number of observed reflections decreases, possibly as a result of continuous structural transformations. Above 10 GPa, new peaks appear indicating the presence of an additional polymorph. The low- and high-pressure phases coexist in the range 10–18 GPa. Similar patterns were collected with no pressure medium to about 22 GPa (Fig. 2). Unlike in the paraffin oil, splittings of some reflections are noticeable at higher pressures. All the transformations are reversible upon decompression with large hysteresis (Fig. 3). Broadening of the observed peaks due to non-hydrostatic effects precluded any reliable structural analysis of the pressure-induced phases of lithium carbonate.

The sample of Li_2CO_3 was annealed at 10 GPa in a diamond anvil cell loaded with Li_2O as a mineralizer using a YAG laser in order to obtain better quality powder X-ray patterns for structural analysis. Fig. 4 shows selected powder X-ray diffraction patterns of the $Li_2O + Li_2CO_3 + Pt$ mixture at different pressures before and after laser annealing. In the pattern collected at 10 GPa before the annealing, both the low- and high-pressure polymorphs of Li_2CO_3 can be observed (compare Figs. 1 and 2). After the annealing, there is no evidence for any products of the reaction between Li_2O and Li_2CO_3 at these pressure conditions and all

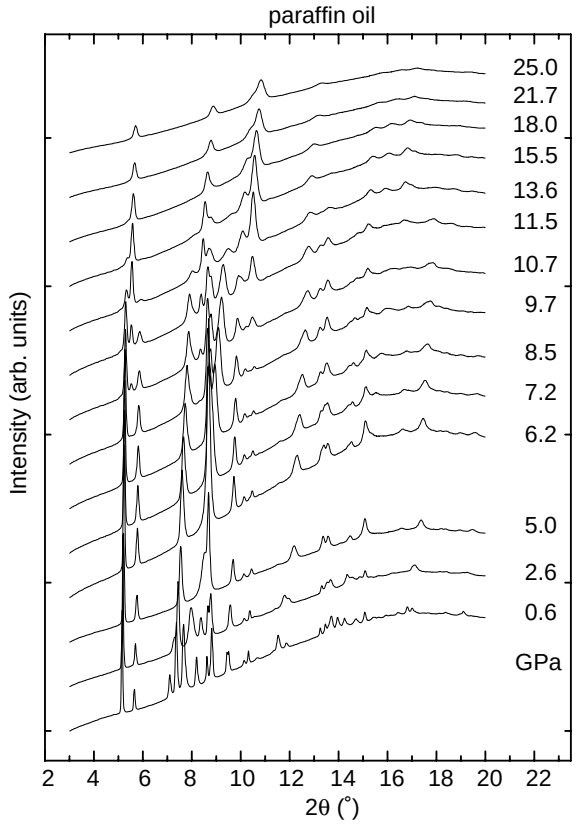

Fig. 1. Selected powder X-ray patterns of Li_2CO_3 collected in a diamond anvil cell upon compression at room temperature with paraffin oil as a pressure medium, $\lambda = 0.3738$ Å.

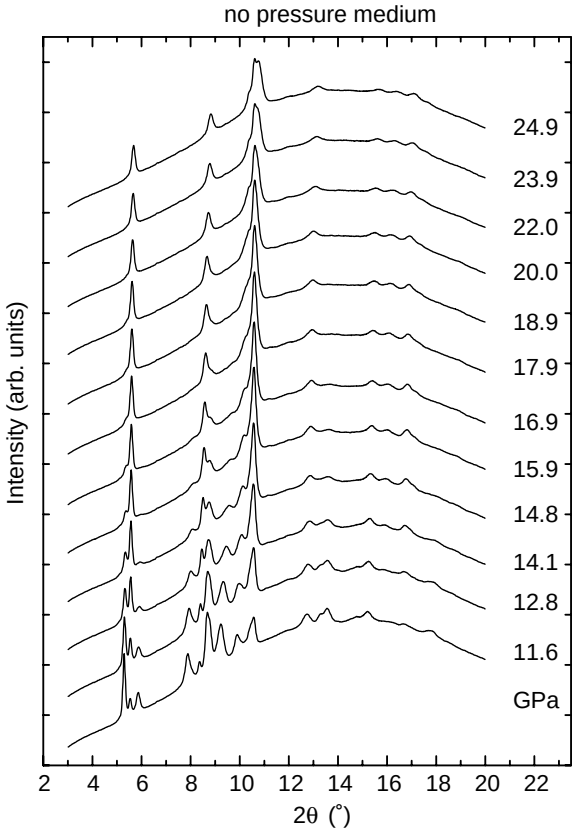

Fig. 2. Selected powder X-ray patterns of Li_2CO_3 collected in a diamond anvil cell upon compression at room temperature with no pressure medium, $\lambda = 0.3738$ Å.

X-ray reflections could be assigned to Li_2O antifluorite, black Pt, and the high-pressure modification of Li_2CO_3 that was previously mixed with the $C2/c$ polymorph above 10 GPa in diamond cells loaded either with paraffin oil or with no pressure medium (compare Figs. 1–3). The pattern of the decompressed sample again shows the low-pressure phase of lithium carbonate (compare Figs. 1–3). Synthesis runs on pure Li_2CO_3 at different pressure, temperature, and time conditions using the multi-anvil apparatus also demonstrate that the new pressure-induced phase is not quenchable (Fig. 5). No decomposition products of lithium carbonate are detected in all our diamond cell and multi-anvil experiments carried out for this study.

After close inspection of the pattern for the $Li_2O + Li_2CO_3 + Pt$ mixture annealed at 10 GPa (Fig. 4), 12 X-ray reflections were assigned to the new high-pressure polymorph of lithium carbonate. They were indexed by the program Treor [16,17] on a hexagonal cell with $a = 4.475(1)$ and $c = 5.140(4)$ Å, $M(12) = 40$ (av. eps. 0.0000132), $F(12) = 72.0$ (0.004919,34). The volume of the unit cell, $V = 89.08$ Å^3, suggested that the Z parameter is equal to 2 with a calculated density $d = 2.76$ g/cm^3. This hexagonal cell was used in the program Endeavour [18] for structure solution with the global minimization method without any bias towards fitting the diffraction pattern or potential functions. The program was run in space group $P1$ and the unit cell contained four Li^+ cations and two rigid planar CO_3^{2-} bodies, for which the molecular internal coordinates were taken from Ref. [11]. The evidence for a presence of undistorted CO_3^{2-} anions was provided by infrared spectroscopy measurements at high pressures [19] showing that internal vibrational modes of the planar carbonate group are unperturbed in the new pressure-induced phase of Li_2CO_3. The space group search and assignment [20] for the obtained solutions with the program Endeavour [18] yielded the crystal structure in space group $P6_3/mcm$ ($Z = 2$). In this structural model, the Li, C, and O atoms occupy the $4d$, $2a$, and $6g$ sites, respectively. The only variable positional parameter is the x coordinate for the oxygen atom at the site $6g$ $(x, 0, 1/4)$. The calculated x parameter was equal to 0.28763.

Fig. 6 shows the Rietveld refined pattern with the three Li_2CO_3, Li_2O, and Pt phases using the program GSAS [21]. The background was fitted with the shifted Chebyshev function (18 points) and not refined [22]. The isotropic U_i/U_e100 thermal parameters for the Li, C, and O atoms in the high-pressure phase of Li_2CO_3 were

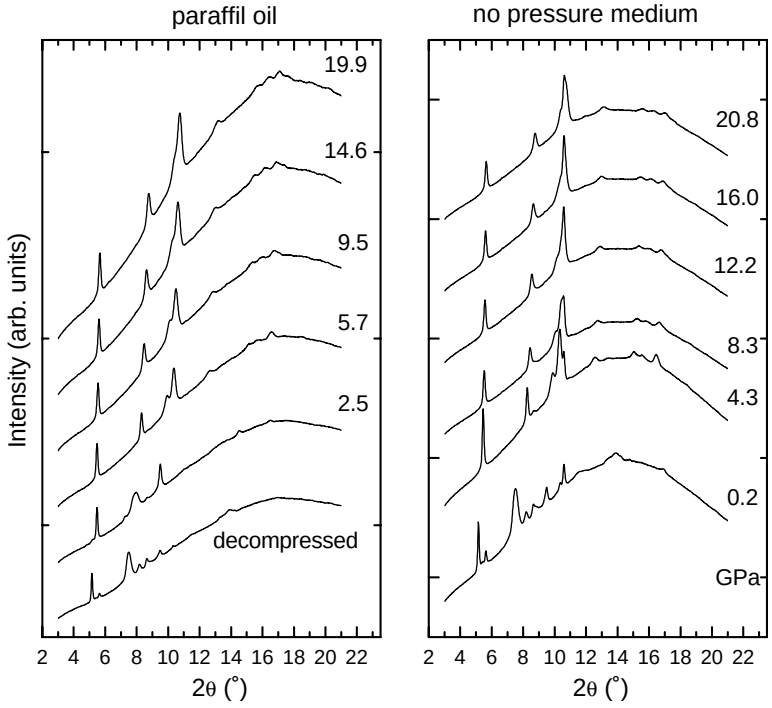

Fig. 3. Selected powder X-ray patterns of Li_2CO_3 collected in diamond anvil cells upon decompression at room temperature with paraffin oil as a pressure medium (left) or with no pressure medium (right), $\lambda = 0.3738$ Å.

all set to 1.5. The refined parameters were: the fractional x atomic coordinate of the O atom in Li_2CO_3 ($P6_3/mcm$, $Z = 2$), the Stephens profile functions for each of the three phases with terms to account for the reflection anisotropic broadening, an overall intensity scaling factor, three parameters for phase fractions, three sets of cell parameters, and a zero shift. The atomic coordinates and selected interatomic distances for the high-pressure polymorph of Li_2CO_3 are given in Table 1. The calculated pattern [23] with the Endeavour structural model for Li_2CO_3 (the fractional coordinate for the O atom is $x_O = 0.288$) is compared with the measured one at 25.0 GPa (paraffin oil as a pressure medium) in Fig. 7.

The crystal structure of the pressure-induced polymorph of Li_2CO_3 ($P6_3/mcm$, $Z = 2$) is shown in Fig. 8. The carbonate groups are in a staggered configuration along the c-axis, reminiscent of the parent $C2/c$ structure [11]. The C–C shortest distance is 2.563 Å at 10 GPa (Table 1), while it is 3.167 Å in the monoclinic modification ($C2/c$, $Z = 4$) at ambient pressure [11]. Unlike in $CaMg(CO_3)_2$, aragonite $CaCO_3$, and $BaMg(CO_3)_2$ for which density functional theory calculations indicated that the aplanarity of CO_3^{2-} anions is a ground state property [24], no aplanar deformation of this anion is noticeable in hexagonal Li_2CO_3. In fact, no distortion of the CO_3^{2-} group is allowed by symmetry. A characteristic feature of this new structure is that the carbonate anions are stacked alternating with the lithium atoms in a distorted octahedral coordination (Table 1, Figs. 8 and 9). Two columns of face-shared octahedra around the Li atoms along the c-axis are linked through octahedral edges. The oxygen atoms are coordinated to one carbon atom and four lithium atoms to form a distorted square pyramid (Table 1, Fig. 10). The major difference between this structure and the hexagonal aristotype ($P6_3/mmc$, $Z = 2$) of other alkali metal carbonates Me_2CO_3 (Me: Na, K, Rb, Cs) is that in the latter the columns of face-shared octahedra around the metals are interconnected by the carbonate groups [12,13].

The tetrahedral coordination of the lithium atoms in monoclinic Li_2CO_3 ($C2/c$, $Z = 4$) also occurs in all three α ($P1$, $Z = 9$), β ($P\bar{6}$, $Z = 9$), and γ ($PP\bar{6}$, $Z = 3$) phases of $LiNaCO_3$ [25]. On the other hand, the structure of the phases in the Li_2CO_3–K_2CO_3 system ($P2_1/n$, $Z = 4$) is composed of distorted face- and edge-sharing LiO_5 and KO_9 coordination polyhedra which are arranged in a layered manner and are connected by carbonate anions [26]. Four Li–O distances are between 1.962 and 2.067 Å, while the additional one is 2.182 Å. The omission of the latter gives a distorted oxygen tetrahedron, in which the Li atom occupies a position almost on one of the tetrahedron faces. Thus, the pressure-induced *tetrahedral→octahedral* coordination change around the Li atoms in Li_2CO_3 during the $C2/c \rightarrow P6_3/mcm$ transformation would correspond to a chemical Li substitution by a heavy alkali metal at ambient

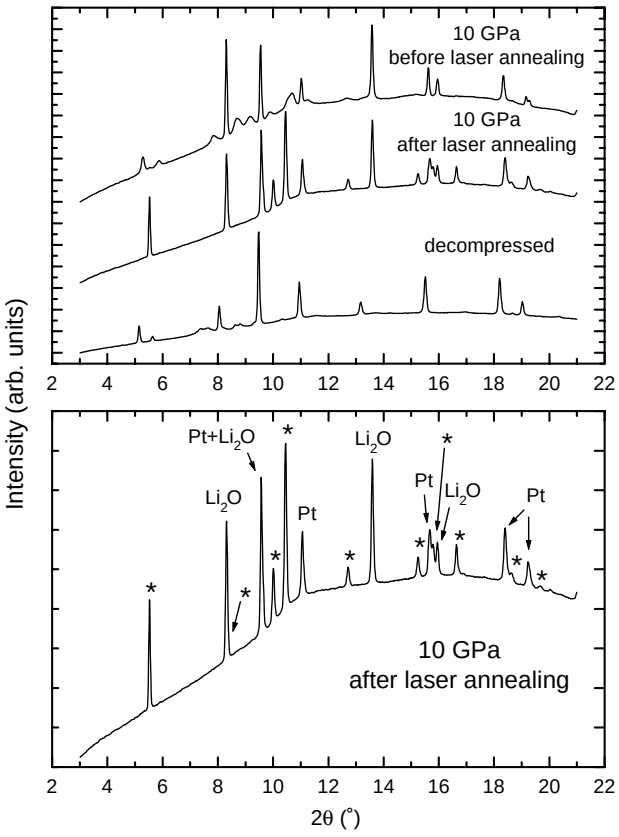

Fig. 4. Selected powder X-ray patterns of the $Li_2CO_3 + Li_2O + Pt$ mixture measured at different pressures and room temperature before and after laser annealing, $\lambda = 0.3738$ Å. The figure at the bottom shows the details of the pattern collected at 10 GPa after laser annealing. The peaks due to Li_2O antifluorite and Pt are explicitly labeled. The major reflections due to a new high-pressure phase of Li_2CO_3 are marked with stars.

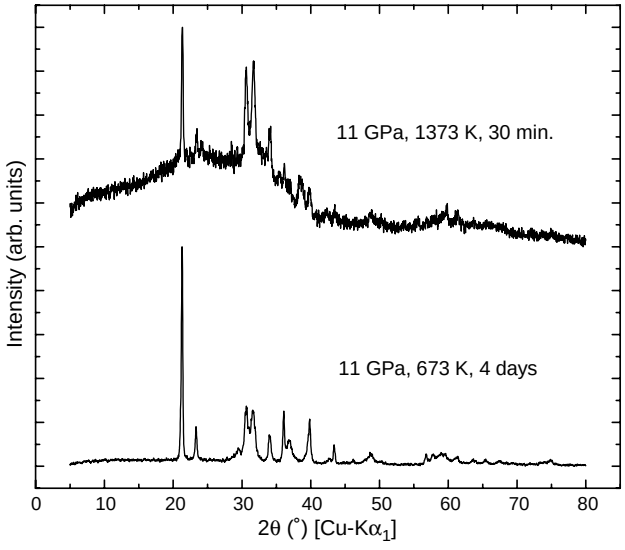

Fig. 5. Powder X-ray diffraction patterns of Li_2CO_3 recovered to ambient from different pressure, temperature, and time conditions in a multi-anvil apparatus (Cu$K\alpha_1$).

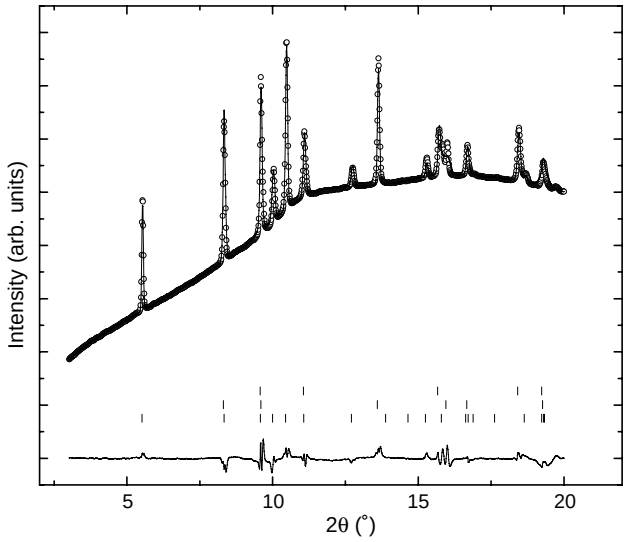

Fig. 6. Observed, calculated, and difference powder X-ray patterns of the $Li_2CO_3 + Li_2O + Pt$ mixture at 10 GPa after laser annealing, $\lambda = 0.3738$ Å. The bottom, middle, and top ticks mark the positions of Bragg reflections for Li_2CO_3 ($P6_3/mcm$, $a = 4.4568(2)$ Å, $c = 5.1254(6)$ Å), Li_2O ($Fm\bar{3}m$, $a = 4.4486(2)$ Å), and Pt ($Fm\bar{3}m$, $a = 3.8613(2)$ Å), respectively—$R(F^2) = 21.2\%$. The residuals $R_{wp} = 1.86\%$ and $R_p = 1.38\%$, whose definitions are given in the GSAS manual [23], are calculated only for the Bragg contribution to the diffraction patterns.

Table 1
Structural data obtained for Li_2CO_3 from a full Rietveld refinement of the pattern collected at 10 GPa after laser annealing—$P6_3/mcm$ ($Z = 2$), $a = 4.4568(2)$ Å, $c = 5.1254(6)$ Å

Atom	Site	x	y	z
Li	*4d*	1/3	2/3	0
C	*2a*	0	0	1/4
O	*6g*	0.2911(4)	0	1/4
Selected distances (Å)				
Li–O	(6 ×)	2.0403(9)		
Li–Li	(2 ×)	2.5627(3)		
	(2 ×)	2.5729(1)		
Li–C	(2 ×)	2.8746(1)		
	(2 ×)	2.8743(1)		
C–O	(3 ×)	1.298(2)		
C–C[a]		2.563		
O–O[a]	(3 ×)	2.247		
	(6 ×)	2.751		
	(3 ×)	2.872		
	(3 ×)	3.168		

Estimated standard deviations are given in parentheses.
[a] Calculated with the program PowderCell [22].

pressure. A comparative study of compressibilities of different alkali metal carbonates is in preparation [19].

The formation of the hexagonal phase of Li_2CO_3 above 10 GPa could explain the observation that at lower pressures the number of observed X-ray reflections for the $C2/c$ polymorph decreases (Fig. 1). As inferred from vibrational spectroscopy investigations

[19], the transition associated with the increase of the coordination around the Li atoms involves in fact a sequence of intermediate stages with different distribution of the Li atoms in the available sites of the (pseudo)hexagonal lattice and different relative orientations of the CO_3^{2-} groups. The resulting structure ($P6_3/mcm$, $Z = 2$) with the carbonate groups in a staggered configuration and with two columns of face-shared octahedra around the Li atoms along the c-axis linked through octahedral edges is not stable upon decompression so that the low-pressure polymorph of Li_2CO_3 is recovered at ambient conditions (Figs. 3–5). On the other hand, the peak splittings observed above about 22 GPa under non-hydrostatic conditions (Fig. 2)

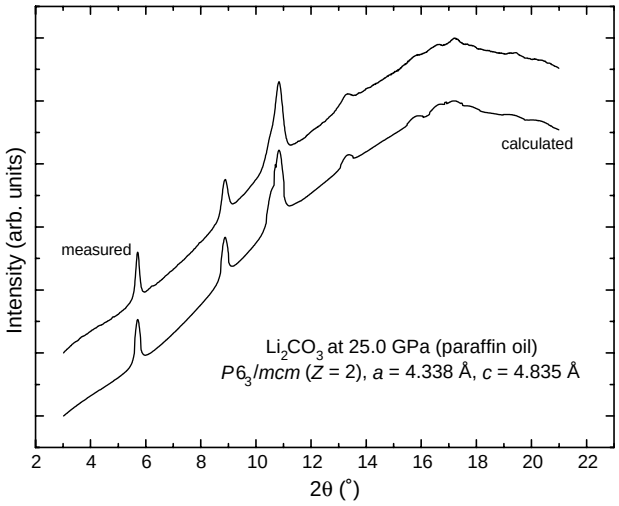

Fig. 7. Comparison of the measured and calculated (with the program PowderCell [22]) powder patterns of Li_2CO_3 at 25.0 GPa in paraffin oil as a pressure medium—$P6_3/mcm$, $a = 4.338$ Å, $c = 4.835$ Å, $x_O = 0.288$.

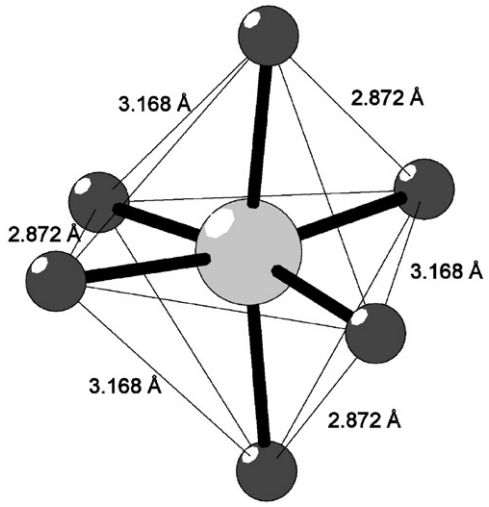

Fig. 9. Distorted octahedron around the Li atom (the light gray symbol). Two sets of long distances among the O atoms (the dark gray symbols) are indicated—2.872 and 3.168 Å (see Table 1).

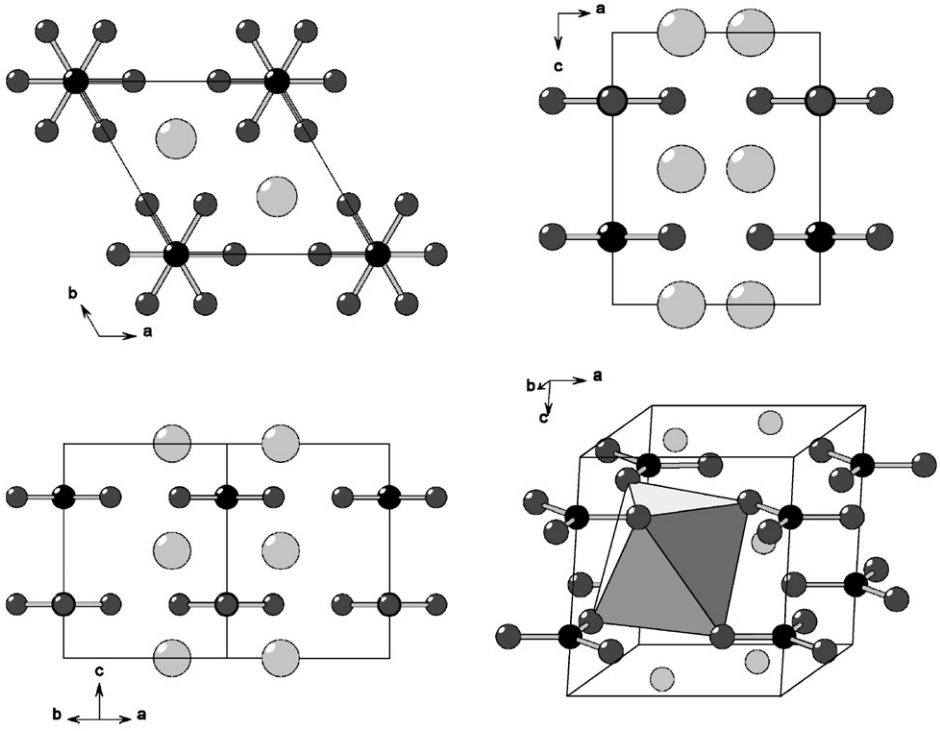

Fig. 8. Crystal structure of the high-pressure phase of Li_2CO_3 ($P6_3/mcm$, $Z = 2$) in different projections. Light gray, black, and medium gray symbols represent the Li, C, and O atoms, respectively. A distorted octahedron around one of the lithium atoms is drawn.

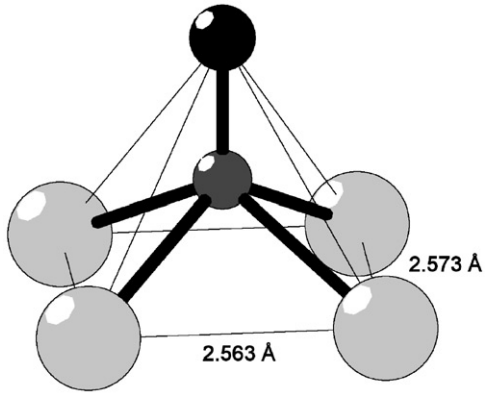

Fig. 10. Square pyramid around the O atom (the dark gray symbol). Two non-equivalent distances among the Li atoms (the light gray symbols) are indicated (see Table 1). The black symbol stands for the C atom.

could result from orthorhombic or monoclinic distortions of the hexagonal lattice, for instance, to accommodate deformations of the carbonate groups and/or repulsive interactions between the neighboring anions, e.g. the simplest *translationengleiche* subgroup of $P6_3/mcm$ is space group *Cmcm*. The conclusion of this study is that upon compression up to about 25 GPa lithium carbonate does not transform to any crystal structures derived from the hexagonal aristotype ($P6_3/mmc$, $Z = 2$) of other alkali metal carbonates Me_2CO_3 (*Me*: Na, K, Rb, Cs) at ambient conditions [12,13].

Acknowledgments

We thank R. Dinnebier and G. Vajenine for their critical comments on the manuscript.

References

[1] Y.N. Pal'yanov, A.G. Sokol, Y.M. Borzdov, A.F. Khokhryakov, N.V. Sobolev, Nature 400 (1999) 417.
[2] L. Sun, W. Wu, Y. Zhang, W. Wang, J. Mater. Res. 14 (1999) 631.
[3] Y.N. Pal'yanov, A.G. Sokol, Y.M. Borzdov, A.F. Khokhryakov, Lithos 60 (2002) 145.
[4] A.G. Sokol, A.A. Tomilenko, Y.N. Pal'yanov, Y.M. Borzdov, G.A. Pal'yanova, A.F. Khokhryakov, Eur. J. Mineral. 12 (2000) 367.
[5] Y.N. Pal'yanov, A.G. Sokol, Y.M. Borzdov, A.F. Khokhryakov, A.F. Shatsky, N.V. Sobolev, Diamond Relat. Mater. 8 (1999) 1118.
[6] L. Sun, M. Akaishi, S. Yamaoka, J. Cryst. Growth 213 (2000) 411.
[7] J.-W. Kim, H.-G. Lee, Metall. Mater. Trans. B 32 (2001) 17.
[8] A.P. Hammersley, S.O. Svensson, M. Hanfland, A.N. Fitch, D. Häusermann, High Pressure Res. 14 (1996) 235.
[9] H.K. Mao, J. Xu, P.M. Bell, J. Geophys. Res. 91 (1986) 4673.
[10] D. Walker, M.A. Carpenter, C.M. Hitch, Am. Mineral. 75 (1990) 1020;
D.C. Rubie, Phase Transitions 68 (1999) 431.
[11] H. Effenberger, J. Zemann, Z. Kristallogr. 150 (1979) 133.
[12] B. Feldmann, M. Jansen, Z. Kristallogr. 215 (2000) 343.
[13] I.P. Swainson, M.T. Dove, M.J. Harris, J. Phys.: Condens. Matter 7 (1995) 4395.
[14] M.J. Harris, E.K.H. Salje, J. Phys. : Condens. Matter 4 (1992) 4399.
[15] H.Y. Becht, R. Struikmans, Acta Crystallogr. B 32 (1976) 3344.
[16] P.-E. Werner, L. Eriksson, M. Westdahl, J. Appl. Crystallogr. 18 (1985) 367.
[17] R. Shirley, The CRYSFIRE System for Automatic Powder Indexing: User's Manual, The Lattice Press, 41 Guildford Park Avenue, Guildford, Surrey GU2 7NL, England, 2000.
[18] H. Putz, J.C. Schön, M. Jansen, J. Appl. Crystallogr. 32 (1999) 864.
[19] L. Farina, et al., in preparation.
[20] A. Hannemann, R. Hundt, J.C. Schön, M. Jansen, J. Appl. Crystallogr. 31 (1998) 922.
[21] A.C. Larson, R.B. von Dreele, GSAS: General Structure Analysis System, Los Alamos National Laboratory, 2000.
[22] B.H. Toby, J. Appl. Crystallogr. 34 (2001) 210.
[23] W. Kraus, G. Nolze, CPD Newsletter no. 20, International Union of Crystallography, 1998.
[24] B. Winkler, J. Zemann, V. Milman, Acta Crystallogr. B 56 (2000) 648.
[25] S.G. Zhukov, A.V. Yatsenko, V.V. Chernyshev, V.A. D'yakov, R. Le Roux, H. Schenk, Z. Kristallogr. 214 (1999) 255.
[26] Y. Idemoto, J.W. Richardson Jr., N. Koura, S. Kohara, C.-K. Loong, J. Solid State Chem. 128 (1997) 156;
Y. Idemoto, J.W. Richardson Jr., N. Koura, S. Kohara, C.-K. Loong, J. Phys. Chem. Solids 59 (1998) 363;
A. Kirfel, H. Euler, B. Barbier, E. Hägele, H. Klapper, Z. Kristallogr. 215 (2000) 744.